ISSN 1070-4272, Russian Journal of Applied Chemistry, 2017, Vol. 90, No. 12, pp. 2019−2027. © Pleiades Publishing, Ltd., 2017.

VARIOUS TECHNOLOGICAL PROCESSES

Preparation of Novel Coumarin Cyclic Polymer/Montmorillonite Based Nanocomposites[1]

A. Kurt* and O. K. Topsoy

Adiyaman University, Adiyaman, 02040 Turkey
**e-mail: adnkurt@gmail.com*

Received December 21, 2017

Abstract—In present study, the synthesis, characterization, and thermal properties of novel coumarin cyclic polymer poly(3-benzoyl coumarin-7-yl-methacrylate) polymer/montmorillonite based nanocomposites were performed. At the characterizations of nanomaterials FTIR, XRD, DSC and TGA techniques were used. It was determined from XRD measurements that the morphologies of nanocomposites were shifted from exfoliated type to intercalated type when the clay ratio in the coumarin polymer matrix was increased from 1 to 5% level. From DSC analysis, a partial increasing at the glass transition temperatures of nanocomposites was observed related to clay ratios. On the other hand, a positive correlation was observed between the clay ratio and thermal stability of nanomaterials from TGA analysis. Also, the increasing of decomposition temperatures of nanocomposites according to homopolymer was recorded to be 9–17°C.

DOI: 10.1134/S1070427217120199

As a result of the dispersing of different additives into polymers, some changes are observed at the properties of these materials. In particular, when the nano-sized additive elements are distributed to the polymer matrix, significant developments have been performed in the properties of those nanomaterials [1]. One of the most important of these nanomaterials is clay-reinforced nanocomposites. So, polymer-clay nanocomposites are widely preferred and used due to many advantages such as easy preparing, achieving high success in the targeted properties, easy availability, etc. [2]. When the polymer clay nanocomposites are compared to neat polymers, they exhibit advanced physical, mechanical and chemical properties such as mechanical strength, electrical resistance, dielectric property, thermal behavior, rheological, gas barrier, and flame retardant [3–13]. These properties generally change according to the distribution pattern of clay in the polymer matrix [4].

On the other hand, a large number of polymers with different reactive functional groups have successfully synthesized and tested todays. These polymers are used in specific applications because of not only their macromolecular properties but also their functional properties [14]. In the class of these polymers, the coumarin-derived polymers belonging to the group of polyphenolic compounds are one of the leading members of reactive functional polymers. As is known, coumarins belong to the family of lactones in the class of oxygen heterocyclic compounds [15]. They are also known as 2*H*-chromen-2-one or 1-benzopyran-2-one consist of fused pyrone and benzene rings with the pyrone carbonyl group at second position [16]. These compounds are widely occurring in the nature and isolated from plants as well as the synthesis may be well performed in the laboratory by various processes [15]. Coumarins have also intensive π-conjugated bonds in their structures and this property makes them very popular for versatile applications in various fields of science and technology [17]. Therefore, coumarins and derivatives exhibit significant photophysical and spectroscopic properties [16] and they have been extensively investigated for electronic and photonic applications such as electro-optical materials, organic-inorganic hybrid materials,

[1] The text was submitted by the authors in English.

Scheme 1. Synthesis of 3-benzoyl-7-hydroxy coumarin.

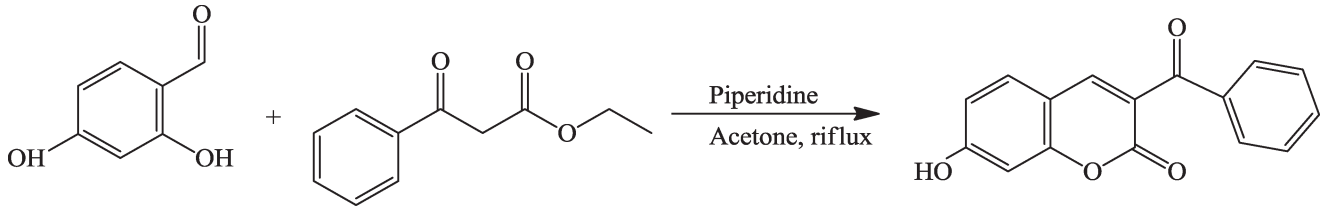

liquid crystal materials, light storage/energy transfer materials [18–22]. Therewithal, these compounds are naturally found, they have also attracted scientific interest due to their important biochemical properties such as antibacterial, antibiotic, antimitotic, antiviral, antitumor, antifungal and antioxidant properties [23–29].

Although some papers been performed to synthesize and examine various properties of small or monomeric coumarin derivatives [30,31], very little attention has been paid to coumarin polymers [32]. In recent years, several works have been reported on the investigation of various properties of coumarin derived polymers [16,33,34]. Within our literature knowledge, however, none of the papers on these polymers are about the coumarin containing polymer/organoclay nanocomposites except of our previous study [35]. With this view, the synthesis of novel coumarin derived polymer/clay nanocomposites based poly(3-benzoyl coumarin-7-yl-methacrylate) polymer reinforced with various contents of organoclay is under taken in current work. The prepared coumarin monomer and polymer are spectrally characterized by FTIR, ^{1}H NMR and ^{13}C NMR techniques while, at the characterization of clay nanocomposites, FTIR and XRD measurements are used. The influence of organoclay on the thermal behaviors of present polymer is studied by means of thermogravimetric analysis (TGA). The obtained results showed a positive relation between the amount of added organoclay phase and thermal stability of nanocomposites.

EXPERIMENTAL

A Perkin Elmer Spectrum 100 was used to obtain the infrared spectra of the nanocomposites. NMR spectra (^{1}H NMR, ^{13}C NMR) were recorded on a Bruker 300 MHZ NMR spectrometer. XRD patterns were recorded at room temperature using Rigaku RadB-DMAX II X-Ray Diffractometer equipped with a CuK_{α} radiation (λ = 0.15418 nm) and Ni filter. Thermogravimetric analysis was conducted on a Seiko SII 7300 TG/DTA under nitrogen flow from 25°C to 500°C at the heating rate of 10°C/min. A Perkin Elmer DSC 8000 was used to examine the glass transition temperature of the nanocomposites. Samples were heated from 25 to 200°C at a rate of 20°C/min under nitrogen atmosphere.

Nanomer® I.28E (25–30 wt % trimethyl stearyl ammonium) was purchased from Sigma–Aldrich, which used as organomodified clay (OMMT). The reagents of 2,4-dihydroxybenzaldehyde, ethyl benzoyl acetate, piperidine, triethylamine, methacryloyl chloride and the solvents of chloroform, acetone, methanol, ethanol, tetrahydrofuran (THF), *N,N*-dimethylformamide (DMF) were purchased from Sigma-Aldrich. Azobisisobutyronitrile (AIBN) was obtained from Merck, and it was purified by dissolving in chloroform and recrystallizing from ethanol just before polymerization.

Synthesis of 3-benzoyl-7-hydroxy coumarin was performed as following: 2,4-dihydroxybenzaldehyde (2.762 g), ethyl benzoyl acetate (3.844 g), three drops of piperidine and 50 mL of acetone were dissolved in a three neck flask. The mixture was stirred on a magnetic stirrer for 2 hours. After this, the organic crude product was precipitated in excess methanol, filtered and dried, respectively. The result compound 3-benzoyl-7-hydroxy coumarin was purified by crystallization from ethanol. The synthesis scheme was shown in Scheme 1. FTIR (cm^{-1}: the most characteristic bands): 3171 (–OH stretching), 3062–2930 (aromatic C–H stretching), 2900–2825 (aliphatic C–H stretching), 1682 (lactone C=O stretching), 1650 (lactone aliphatic C=C stretching), 1609 (aromatic C=C stretching).

^{1}H NMR (DMSO, δ, ppm): 10.98 (–OH proton), 8.35 (lactone =CH–proton), 7.88–6.79 (aromatic =CH–protons).

^{13}C NMR (DMSO, δ, ppm): 191.95 (benzoyl ketone carbonyl carbon), 163.28 (lactone carbonyl carbon), 158.37, 156.60, and 146.80 (ipso carbons next to hydroxyl group, lactone oxygen and benzoyl carbonyl carbon,

Scheme 2. Synthesis of 3-benzoyl coumarin-7-yl-methacrylate (BCMA) monomer.

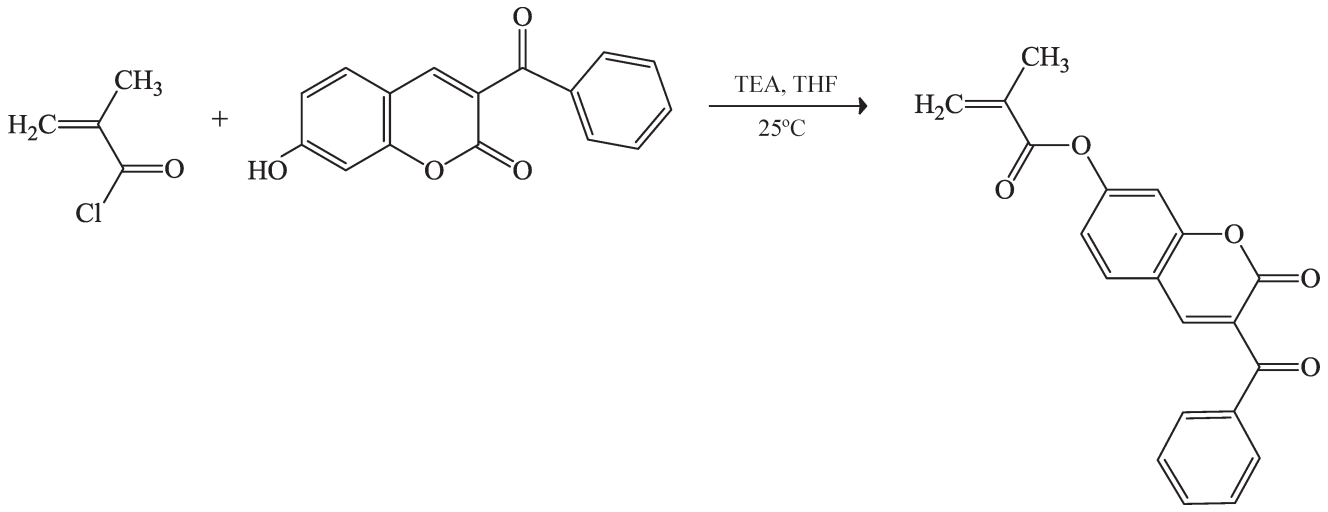

respectively), 136.73–102.04 (aromatic and aliphatic C=C carbons).

To synthesize 3-benzoyl coumarin-7-yl-methacrylate monomer (BCMA), 3-benzoyl-7-hydroxy coumarin (1.76 g, 8.70 mmol), TEA (1.20 g, 8.70 mmol) and THF (75 mL) were added into a reaction flask. Methacryloyl chloride (0.91 g, 8.70 mmol) was dropwised to this mixture and stirred on the magnetic stirrer for 12 h at room temperature. After the reaction was completed, the mixture was filtered and the THF was removed in vacuum. The organic phase was taken up in chloroform and extracted several times with diluted NaOH solution of 3%. The chloroform phase was dried over anhydrous $MgSO_4$ overnight. The mixture was filtered and the solvent was removed in vacuum. The reaction mechanism of 3-benzoyl coumarin-7-yl-methacrylate monomer was shown in Scheme 2.

FTIR (cm^{-1}: the most characteristic bands): 3122–3034 (aromatic C–H stretching), 2982–2846 (aliphatic C–H stretching), 1737 (methacrylate C=O stretching), 1710 (coumarin benzoyl C=O stretching), 1682 (lactone C=O stretching), 1656 (lactone aliphatic C=C stretching), 1638 (vinylic C=C stretching).

^{1}H NMR (DMSO, δ, ppm): 8.45 (lactone =CH– proton), 7.97–7.28 (aromatic =CH– protons), 6.35 and 5.97 (vinyl $=CH_2$ protons), 2.03 (CH_3 protons next to vinyl group).

^{13}C NMR (DMSO, δ, ppm):191.60 (benzoyl ketone carbonyl carbon), 164.71 (methacrylate ester carbonyl carbon), 157.81 lactone carbonyl carbon), 154.83, 154.28 and 145.08 (ipso carbons next to lactone oxygen, methacrylate ester carbonyl and benzoyl carbonyl carbon, respectively), 136.06–110.19 (aromatic and aliphatic C=C carbons), 17.95 (–CH_3 carbon next to vinyl group).

Then, a free radical polymerization method was applied to polymerize the 3-benzoyl coumarin-7-yl-methacrylate monomer (BCMA). For this purpose, monomer (2.0 g), DMF solvent (10 mL) and AIBN initiator (0.12 g, 6 wt % of the monomer) were added into a polymerization tube and degassed with argon for 10 minutes. After that, polymerization was carried out 60°C for 48 h. The polymer was precipitated in ethanol, filtrated and dried overnight in a vacuum oven at 40°C. Synthesis of poly(3-benzoyl coumarin-7-yl-methacrylate) was illustrated in Scheme 3.

FTIR (cm^{-1}: the most characteristic bands): 3164–3038 (aromatic C–H stretching), 2995–2888 (aliphatic C–H stretching), 1737 (methacrylate C=O stretching), 1731 (coumarin benzoyl C=O stretching), 1696 (lactone C=O stretching), 1662 (lactone aliphatic C=C stretching), 1613 (aromatic C=C stretching).

^{1}H NMR (DMSO, δ, ppm): 8.19 (lactone =CH– proton), 7.78–7.22 (aromatic =CH– protons), 1.69 and 1.45 (methylene and methyl protons on the polymer main chain, respectively).

Finally, the novel nanocomposites of coumarin derived polymer reinforced with various ratios of organoclay (poly(BCMA)/OMMT) were prepared using the solution casting method. For this process, the necessary amounts of organoclay (1%, 3% and 5%) were separately taken

Scheme 3. Synthesis of poly(3-benzoyl coumarin-7-yl-methacrylate) [poly(BCMA)].

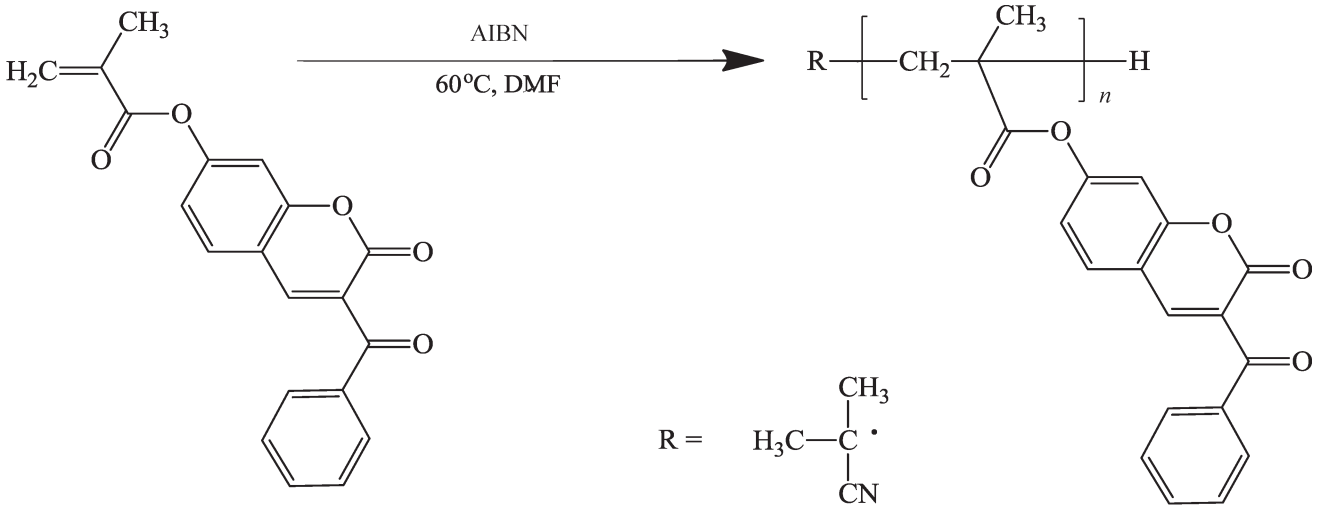

into three balloons (50 mL) and dispersed in 3 mL of DMF, and stirred by magnetic stirrers at room temperature for 48 h. During this period, three separate poly(BCMA) polymer samples (weights of 0.5 g) were also separately dissolved in 3 mL of DMF at room temperature in the other three balloons. Then, these poly(BCMA) polymer/DMF solutions were gradually added into each organoclay/DMF suspensions. The mixtures were stirred for another 48 h with magnetic stirrers at room temperature. After that, the polymer/organoclay mixtures were precipitated in the excess ethanol to isolate from DMF solvent. Then, the prepared nanocomposites were dried in the air atmosphere for 24 h and finally, they were powdered by passing from a sieve with 21 micron mesh.

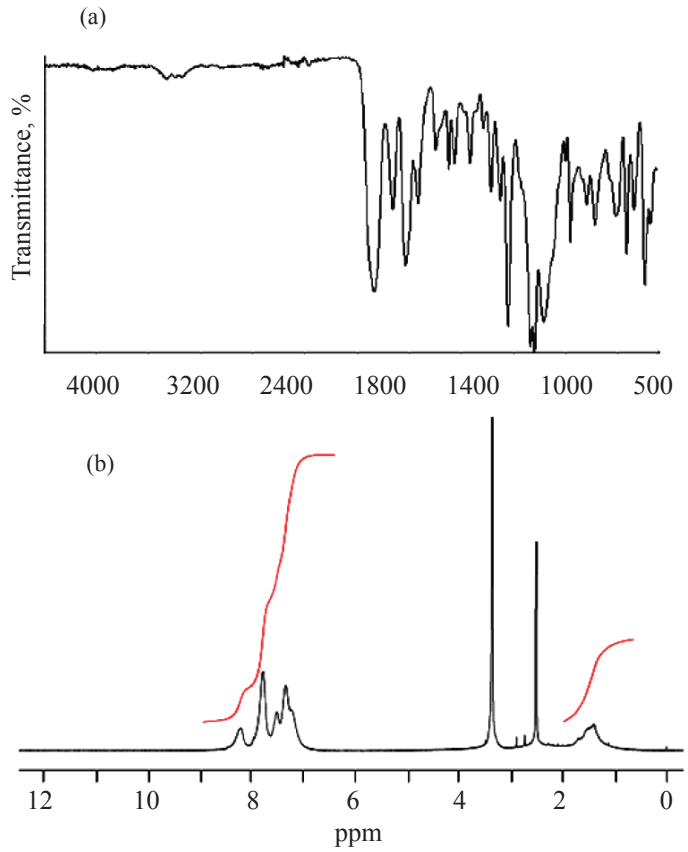

Fig. 1. (a) FTIR and (b) ^{1}H NMR spectra of poly(BCMA) polymer.

RESULTS AND DISCUSSION

We have spectral characterized the coumarin derived polymer, poly(3-benzoyl coumarin-7-yl-methacrylate). One of the used spectral techniques is FTIR technique. Figure 1a shows FTIR spectrum of polymer in which the most important evidence of performing the polymerization is the disappearing of the absorption attributed to vinylic C=C stretching at 1638 cm^{-1} with the polymerization. In addition to this important changing, the other absorption bands characterizing the coumarin polymer are observed at 3164–3038 cm^{-1} (aromatic C–H stretching), 2995–2888 cm^{-1} (aliphatic C–H stretching), 1737 cm^{-1} (methacrylate C=O stretching), 1731 cm^{-1} (coumarin benzoyl C=O stretching), 1696 cm^{-1} (lactone C=O stretching), 1662 cm^{-1} (lactone aliphatic C=C stretching), 1613 cm^{-1} (aromatic C=C stretching). Also, another spectral technique, ^{1}H NMR spectrum of poly(BCMA) is shown in Fig. 1b. The resonances at 6.35

and 5.97 ppm attributed to the aliphatic $=CH_2$ protons which are characteristic for the monomer vinyl group are not observed. This indicates that the vinylic C=C double bonds in the monomer opened during polymerization and thus, the polymerization has been achieved. Besides, the other signals are also observed at 8.19 ppm (lactone =CH– proton), 7.78–7.22 ppm (aromatic =CH– protons), 1.69 and 1.45 ppm (methylene and methyl protons on the polymer main chain, respectively).

The organomodified clay (OMMT) is characterized with FTIR technique and its spectrum is illustrated in Fig. 2a. Especially, two different signal groups have been seen in this spectrum. One of them characterizes the pristine clay (Na–MMT) units. The most characteristic absorptions of that are for 3620 cm^{-1} OH stretching, 1001 cm^{-1} Si–O stretching, 913 cm^{-1} Al–OH deformation, 797 cm^{-1} silica Si–O stretching, 621 cm^{-1} out of plane Al–O and Si–O stretching, 520 cm^{-1} Al–O–Si deformation. Another signal groups are recorded for the intercalating agent units where the most characteristic bands are 2922–2850 cm^{-1} aliphatic C–H stretching and 1469 cm^{-1} aliphatic C–H shear vibrations. This spectrum containing both of mentioned two signal groups indicates that the organic modification of pristine montmorillonit clay (Na–MMT) with intercalating agent is well performed [36]. For comparison, we have discussed here only the FTIR spectrum of the poly(BCMA)/OMMT: 5% nanocomposite because of its similarity to the FTIR spectra of all other nanocomposites illustrated in Figs. 2b–2d. Also, the FTIR spectrum of neat polymer poly(BCMA) polymer is re-illustrated as Fig. 2e to make comparison easier. The characteristic absorptions for both polymeric and organosilicate units are also available in Fig. 2d. The most characteristic bands observed for poly(BCMA) units are seen in 3096–2888 cm^{-1} (aromatic and aliphatic C–H stretching vibrations), 1735 cm^{-1} (ester carbonyl stretching), 1664 cm^{-1} (lactone C=C stretching), 1612 cm^{-1} (aromatic C=C stretching). On the other hand, especially, the absorption band characteristic for clay and attributed to Si–O stretching shifts 1043 cm^{-1} frequency. Compared to other nanocomposites, a clear increasing at the peak intensity of this absorption has been seen depend on the rate of loading clay. Also, at this spectrum, the absorptions of 919, 627, and 522 cm^{-1} are recorded for Al–OH deformation, Al–O/Si–O out of plane vibration and Al–O–Si deformation, respectively. In the FTIR spectra recorded for all polymer–clay nanocomposites, the adsorptions attributed to both organomodified clay units and coumarin polymer units appears in the same spectrum. From these results, it can be said that the organomodified clay presents in polymer matrix as is reported by Krishna and Pugazhenthi [37].

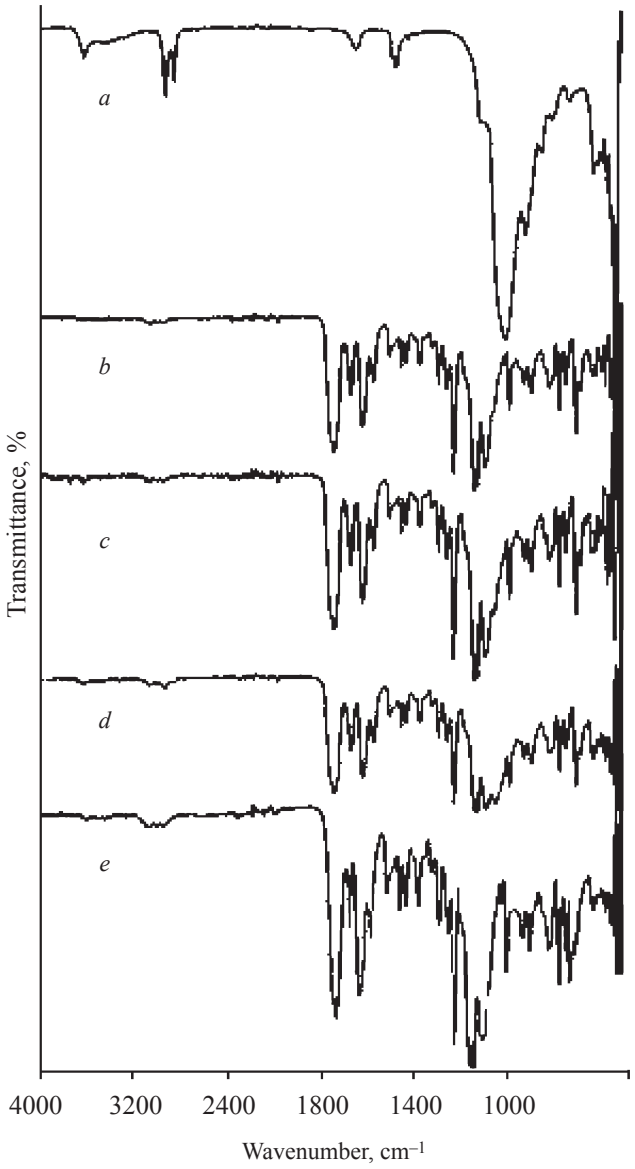

Fig. 2. FTIR spectra of (*a*) organoclay (OMMT), (*b*) poly(BCMA)/OMMT 1%, (*c*) poly(BCMA)/OMMT 3%, (*d*) poly(BCMA)/OMMT 5%, (*e*) neat poly(BCMA).

The structure of clay dispersion in the polymer matrix was determined by XRD analysis depend the *d*-spacing of clay galleries. Especially, two general structures of layered clay dispersion which are intercalated and exfoliated types are seen in the polymer/clay nanocomposites

Thermal behaviors of poly(BCMA)/OMMT nanocomposites

Nanocomposite	*T*, °C[a]	*T*, °C[b]	*T*, °C[c]	Weight loss, % (350°C)	Weight loss, % (400°C)	Weight loss, % (500°C)
Poly(BCMA)	179	321.37	402.79	11.91	46.65	87.02
Poly(BCMA)/OMMT 1%	179.2	330.36	406.39	8.43	41.06	83.02
Poly(BCMA)/OMMT 3%	179.6	338.71	407.75	2.53	38.48	76.16
Poly(BCMA)/OMMT 5%	180.5	337.72	405.76	6.71	41.91	72.88

[a] Glass transition temperature. [b,c] Temperatures at 5% and 50% weight losses, respectively.

[38]. When *d*-spacing (*d*001) of galleries are larger than the pure clay, the intercalated structure is seen for the morphology of nanocomposites, whereas no peak is seen in the XRD curve, in this case, the structure of clay dispersion becomes exfoliated type [37]. The *d*-spacing of clay galleries is calculated using the Bragg's law: $n\lambda = 2d \sin\theta$, where λ is the X-ray wave length (1.5418 Å), *d* is the interlayer distance and θ is the angle of incident radiation.

The wide angel X-ray diffraction curves of novel prepared coumarin derived polymer/clay nanocomposites reinforced with the different clay ratios (1, 3, and 5%) are illustrated in Figs. 3a–3d). The XRD curve recorded for organomodified clay (Fig. 3a), the diffraction angel of clay layers are at 3.9° that corresponds to the basal gallery spacing of 2.27 nm. On the other hand, the *d*-spacing of pristine clay is at higher diffraction angels about ≈9° and also lower basal distances in literature [39, 40]. As is seen in Fig. 3a, the basal spacing of the organomodified clay is significantly expanded with the long alkyl chains and with the volume of the substituent of the intercalating agent [36]. In the XRD curve of the poly(BCMA)/OMMT : 1% nanocomposite containing 1% organoclay content (Fig. 3b), the diffraction angle of 3.9° recorded for the organoclay (OMMT) has been completely disappeared and no diffraction peaks characteristic of OMMT clay have observed in the 2θ–10θ testing range. These result shows that the clay layers in the poly(BCMA)/OMMT : 1% nanocomposite reinforced 1% organoclay exhibits the exfoliation behavior in which the clay layers are completely separated from each other and dispersed in the polymer matrix randomly [37]. On the other hand, in the XRD patterns of poly(BCMA)/clay nanocomposites containing 3% and 5% OMMT, the diffraction peaks are shifted to 3.68° and 3.74° and also, the basal spaces of them are 2.40 nm and 2.36 nm, respectively. The interlayer spaces of both these two nanocomposites have partially increased according to organomodified clay galleries. However, these diffraction peaks have not completely disappeared in the testing range although it has seen a splayed in the peak shapes. As positively associated with high clay contents, the poly(BCMA) polymer chains with bulky coumarin side groups are partially placed between the clay galleries by reducing the present interlayer seconder forces. Since all the interlayer forces have not been removed between the galleries, the clay layers are not separated from each other. Thus, the clays are intercalated in the poly(BCMA) polymer matrix at the ratios of 3 and 5% OMMT. This observation also agrees with the previous observations in the literatures that clays can be intercalated in polymer matrix [4,37].

Figures 4a–4d shows DSC curves of the pure poly(BCMA) homopolymer and its nanocomposites reinforced with clay in various percentages. The glass transition temperatures (T_g) of nanocomposites were given in the table. The pure poly(BCMA) showed a transition at 179°C due to the large coumarin side group and the restriction of polymer chain movement.

This value is agreement with the T_g values recorded for the coumarin-derived polymers in the literature. In a study, Fomine and coworkers reported that the T_g values of some coumarin polymers were shifted in the range of 100–230°C [41]. Venkatesan et al. [32] reported that the copolymer of 7-methacryloyloxy-4-methylcoumarin with butoxyethyl methacrylate (feed composition 80 : 20) showed the T_g at 138°C. In our previous study [35],

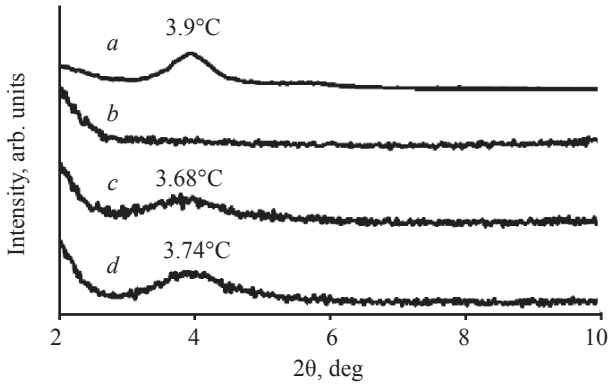

Fig. 3. XRD patterns of (*a*) organoclay (OMMT), (*b*) poly(BCMA)/OMMT 1%, (*c*) poly(BCMA)/OMMT 3%, (*d*) poly(BCMA)/OMMT 5%.

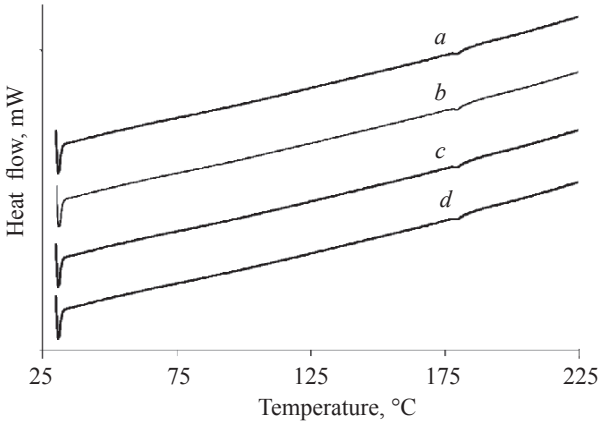

Fig. 4. DSC curves of (*a*) poly(BCMA), (*b*) poly(BCMA)/OMMT 1%, (*c*) poly(BCMA)/OMMT 3%, (*d*) poly(BCMA)/OMMT 5%.

we determined the glass transition temperature of a coumarin derived polymer poly(3-acetylcoumarin-7-yl-methacrylate) to be 176°C.

As can be seen in Figs. 4a–4d, when the organomodified clay ratio in the coumarin derivative poly(BCMA) matrix increased to 5% level, the glass transition temperature also partially increased from 179 to 180.5°C. It was observed that the glass transition temperature of nanocomposites was approximately 1.5°C higher than that of pure poly(BCMA). This partial increasing may be because the movement of poly(BCMA) homopolymer chains are prevented by the sheets of the clay. Thus, the segmental motions of the polymer chains are restricted at the polymer–clay interface due to polymer–clay interaction and thus, the transition temperatures of polymeric nanomaterials increase as described in literature [35–37]. However, the increasing at the T_g of nanocomposites is not at very high levels. As a result, the glass transition temperature values of the poly(BCMA)/OMMT nanocomposite samples have not significantly changed with the clay reinforcements, and show the transitions near that of the pure polymer (179°C). On the other hand, we think that one of the reasons why the glass transition temperature is not sufficiently increased may be that the clay dispersion is not well dispersed in the polymer matrix. In this perspective, similar results on the glass transition temperatures of polymer/organoclay nanocomposites have been seen in the literature. In one study of them reported by Zidelkheir and coworkers [42], they expressed that the T_g of intercalated polystyrene/OMMT nanocomposite prepared by melt intercalative compounding technique was increased 3.3–4°C by the OMMT loading 2% to 10%. They interpreted the reason of that caused by the strong interaction between OMMT and polystyrene which limited the cooperative motions of the polymer chains. In another study, Wang et al. [43] reported the glass transition temperatures of polystyrene–clay (1–5 wt %) nanocomposites were 2.4–6.2°C higher than that of neat polystyrene, which was reasoned by the preventing of segmental motions of the intercalated polymer chains within the clay galleries. In a similar work, Krishna and Pugazhenthi [37] observed that the glass transition temperature of PS/OMMT nanocomposites prepared via solvent blending method at various ratios of organoclay (3–20 wt %) were approximately 7.1–8.6°C higher than that of neat polymer.

Thermal behaviors of novel nanocomposites based coumarin derived poly(BCMA) filled with the organoclay in different ratios are determined by TGA technique, and their thermograms are shown in Figs. 5a–5d compared with each other. Also, their results are given in the table which clearly demonstrates that the thermal decomposition temperatures of poly(BCMA)/clay nanocomposites are higher than that of pure poly(BCMA) homopolymer. When the 5% weight loss at the 10°C min^{-1} heating rate have been chosen for comparison, the thermal decomposition temperature of poly(BCMA) homopolymer and its nanocomposites reinforced with organoclay at the ratios of 1, 3, and 5% are determined as 321.37, 330.36, 338.71, and 337.72°C, respectively. As can be seen from these results, thermal stabilities of nanocomposites are increased by about 9–17°C by loading clay into the coumarin derived polymer matrix. These results also agree with the previous observations in the literatures that the

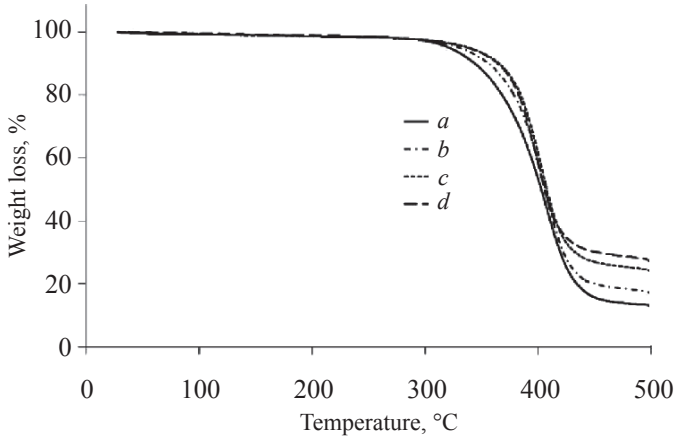

Fig. 5. TGA curves of (*a*) poly(BCMA), (*b*) poly(BCMA)/OMMT 1%, (*c*) poly(BCMA)/OMMT 3%, (*d*) poly(BCMA)/OMMT 5%.

increasing of decomposition temperature to higher values with organoclay loading [35, 37, 39, 44–46]. For example, Qiu and coworkers [45] determined the thermal decomposition temperature of the some PS nanocomposites was 16°C higher than that of pure PS. Krishna & Pugazhenthi [37] found the thermal decomposition temperature of PS/OMMT nanocomposites were 17°C higher than that of pure polymer. Hu et al. [46] reported the decomposition temperature at 10% weight loss was approximately 30°C higher than that of pristine PMMA depending upon the clay content. In another study, Vyazovkin and friends [44] showed that the polystyrene/clay nanocomposites had 30–40°C higher degradation temperature than that of neat polymer under heating conditions.

CONCLUSIONS

Novel polymer/clay nanocomposites based coumarin derived poly(3-benzoyl coumarin-7-yl-methacrylate) reinforced with various ratios of organomodified montmorillonite were prepared by the solution casting method. It was determined from XRD measurements that the morphologies of nanocomposites were shifted from exfoliated type to intercalated type when the clay ratio in the coumarin polymer matrix was increased from 1 to 5% level. A positive correlation was observed between the clay ratio and thermal stability of nanomaterials from TGA analysis. Thermal stabilities of nanocomposites were increased about 9–17°C by loading clay into the polymer matrix. From DSC analysis, a partial increasing at the glass transition temperatures of nanocomposites was observed related to clay ratios.

ACKNOWLEDGMENTS

We wish to thank the Adıyaman University Scientific Research Projects Unit (ADYÜBAP/FFYL2015-0001) for financially supporting this study.

REFERENCES

1. Feldman, D., *J. Macromol. Sci. A.,*, 2013, vol. 50, no. 12, pp. 1241–1249.
2. Utracki, L.A., Sepehr, M., and Boccaleri, E., *Polym. Adv. Technol.*, 2007, vol. 18, no. 1, pp. 1–37.
3. Lerari, D., Peeterbroeck, S., Benali, S. et al., *J. Appl. Polym. Sci.,* 2011, vol. 121: no. 3, pp. 1355–1364.
4. Lee, M.H., Dan, C.H., Kim, J.H. et al., *Polymer,* 2006, vol. 47, no. 12, pp. 4359–4369.
5. Haraguchi, K., *Curr. Opin. Solid State Mater. Sci.,* 2007, vol. 11, no. 3, pp. 47–54.
6. Powell, C.E., and Beall, G.W., *Curr. Opin. Solid State Mater. Sci.,* 2006, vol. 10, no. 2, pp. 73–80.
7. Wang, Y., and Chen, W.C., *Compos. Interface,* 2010, vol. 17, no. 9, pp. 803–829.
8. Qiu, L., and Qu, B., *J. Colloid Interface Sci.,* 2006, vol. 301, no. 2, pp. 347–351.
9. Qiu, L., Chen, W., and Qu, B., *Polymer,* 2006, vol. 47, no. 3, pp. 922–930.
10. Wang, H.W., Chang, K.C., Yeh, J.M., and Liou, S.J., *J. Appl. Polym. Sci.,* 2003, vol. 91, no. 2, pp. 1368–1373.
11. Yeh, J.M., Liou, S.J., Lin, C.G. et al., *J. Appl. Polym. Sci.,* 2004, vol. 92, no. 3, pp. 1970–1976.
12. Kim, M.H., Park, C.I., Choi, W.M. et al., *J. Appl. Polym. Sci.,* 2004, vol. 92, no. 4, pp. 2144–2150.
13. Achilias, D.S., Panayotidou, E., and Zuburtikudis, I., *Thermochim. Acta,* 514, no. 1, pp. 58–66.
14. Patel, H.J., Patel, M.G., Patel, A.K., et al., *Express Polym. Lett.,* 2008, vol. 2, no. 10, pp. 727–734.
15. Nikhil, B., Shikha, B., Anil, P., and Prakash, N.B., *Int. Res. J. Pharmacy (IRJP)*, 2012, vol. 3, no. 7, pp. 24–29.
16. Skowronski, L., Krupka, O., Smokal, V., et al., *Opt. Mater.,* 2015, vol. 47, pp. 18–23.
17. Tasior, M., Kim, D., Singha, S., et al., *J. Mater. Chem.,* 2015, vol. 3, no. 7, pp. 1421–1446.
18. Brun, M.P., Bischoff, L., and Garbay, C., *Angew. Chem. Int. Edit.,* 2004, vol. 43, no.26, pp. 3432–3436.
19. Zhao, L., Loy, D.A., and Shea, K.J., *J. Am. Chem. Soc.,* 2006, vol. 128, no. 44, pp. 14250–14251.
20. Jackson, P.O., O'Neill, M., Duffy, W.L., et al., *Chem.*

Mater., 2001, vol. 13, no. 2, pp. 694–703.

21. Kim, C., Trajkovska, A., Wallace, J.U., and Chen, S.H., *Macromolecules,* 2006, vol. 39, no. 11, pp. 3817–3823.
22. Tian, Y., Akiyama, E., Nagase, Y., et al., *J. Mater. Chem.,* 2004, vol. 14, no. 24, pp. 3524–3531.
23. Soine, T.O., *J. Pharm. Sci.,* 1964, vol. 53, pp. 231–264.
24. Sharma, P., and Pritmani, S., *Indian J. Chem., Sect B,* 1999, vol. 38, no. 9, pp. 1139–1142.
25. Patonay, T., Litkei, G., Bognar, R., et al., *Pharmazie,* 1984, vol. 39, no. 2, pp. 84–91.
26. Shaker, R.M., *Pharmazie,* 1996, vol. 51, no. 3, pp. 148–151.
27. Emmanuel-Giota, A.A., Fylaktakidou, K.C., Hadjipavlou-Litina, D.J., et al., *J. Heterocycl. Chem.,* 2001, vol. 38, no. 3, pp. 717–722.
28. Nofal, Z.M., El-Zahar, M.I., and Abd El-Karim, S.S., *Molecules,* 2000, vol. 5, pp. 99–113.
29. Srivastava, A., Mishra, V., Singh, P., and Kumar, R., *J. Appl. Polym. Sci.,* 2012, vol. 126, no. 2, pp. 395–407.
30. Rabahi, A., Makhloufi-Chebli, M., Hamdi, S.M., et al., *J. Mol. Liq.,* 2014, vol. 195, pp. 240–247.
31. Donovalova, J., Cigan, M., Stankovicova, H., et al., *Molecules,* 2012, 17, no. 3, pp. 3259–3276.
32. Venkatesan, S., Ranjithkumar, B., Rajeshkumar, S., and Anver Basha, K., *Chin. J. Polym. Sci.,* 2014, vol. 32, no. 10, pp. 1373–1380.
33. Essaidi, Z., Krupka, O., Iliopoulos, K., et al., *Opt. Mater.,* 2013, vol. 35, no. 3, pp. 576–581.
34. Zhang, C., Liang, R., Jiang, C., et al., *J. Appl. Polym. Sci.,* 2008, vol. 108, no. 4, pp. 2667–2673.
35. Kurt, A. and Koca, M., *J. Eng. Research*, 2016, vol. 4, no. 4, pp. 46–65.
36. Zhang, W.A., Chen, D.Z., Xu, H.Y. et al., *Eur. Polym. J.,* 2003, vol. 39, no. 12, pp. 2323–2328.
37. Krishna, S.V., and Pugazhenthi, G., *J. Appl. Polym. Sci.,* 2011, vol. 120, no. 3, pp. 1322–1336.
38. Fu, X. and Qutubuddin, S., *Polymer,* 2001, vol. 42, no. 2, pp. 807–813.
39. Kurt, A. and Yılmaz, P., *Kuwait J. Sci*., 2016, 43, no. 2, pp. 172–184.
40. Stoeffler, K., Lafleur, P.G., and Denault, J., *Polym. Eng. Sci.,* 2008, vol. 48, no. 8, pp. 1449–1466.
41. Fomine, S., Rivera, E., Fomina, E., et al., *Polymer,* 1998, vol. 39, no. 15, pp. 3551–3558.
42. Zidelkheir, B., Boudjemaa, S., Abdel, G.M., and Djelloui, B., *Iran. Polym. J.,* 2006, vol. 15, no. 8, pp. 645–653.
43. Wang, H.W., Chang, K.C., Yeh, J.M., and Liou, S.J., *J. Appl. Polym. Sci.,* 2004, vol. 91, no. 2, pp. 1368–1373.
44. Vyazovkin, S., Dranca, I., Fan, X., and Advincula, R., *Macromol. Rapid Commun.,* 2004, vol. 25, no. 3, pp. 498–503.
45. Qiu, L., Chen, W., and Qu, B., *Polym. Degrad. Stabil.,* 2005, vol. 87, no. 3, pp. 433–440.
46. Hu, Y.H., Chen, C.Y., and Wang, C.C., *Polym. Degrad. Stabil.,* 2004, vol. 84, no. 3, pp. 545–553.